

# LOW FIDELITY MODEL FOR HYPERSONIC AEROTHERMOELASTICITY WITH SHOCK IMPINGEMENT AND THERMO-MECHANICAL BUCKLING

Dylan D. Dooner<sup>\*1</sup>, Damon Kirkpatrick<sup>1</sup>, Andrew J. Neely<sup>1</sup>

<sup>1</sup>The University of New South Wales, Canberra,  
 School of Engineering and Technology, Campbell, ACT, 2612, Australia  
 d.dooner@unsw.edu.au

## 1 INTRODUCTION

The focus of this work was the development of a low-cost model with acceptable fidelity. The specific purpose was as a tool to assist the development and analysis of an experimental campaign exploring the role of thermo-mechanical buckling of a clamped-free-clamped-free compliant panel when exposed to an impinging shock.

## 2 EXPERIMENTAL SETUP

The experimental basis for numerical comparison is that of a thin, aluminium panel which is only clamped at the leading and trailing edges. Additionally, a variable incidence shock generator is located above and upstream of the panel and supporting structure, allowing for the exploration of shock impingement effects. Along with the incident shock flow that the top surface is exposed to, the bottom surface is also exposed to flow. The flow that the bottom surface sees is a function of the upwind hammerhead geometry which has compression, streamlined, and expansion faces (i.e., a near-trapezoidal cross-section), and a final small trailing-edge boat-tail. A visualisation of the geometry is provided in Figure 1. The material properties of the aluminium panel are derived from those in MMPDS-2025.

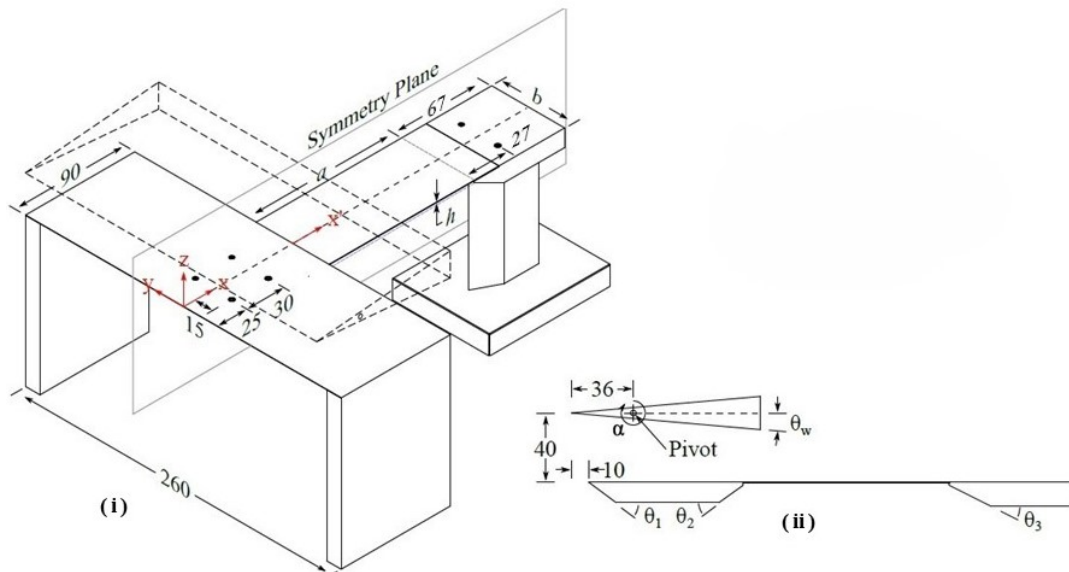


Figure 1: Experimental geometry. (i) Isometric view, (ii) Side profile. Linear dimensions in millimetres.

The aerodynamic environment for the test article and supporting structures is that of the Mach 6 condition of the free-piston compression Ludwig tube located at the University of Southern

Queensland (TUSQ). This facility allows for nominal run durations at the Mach 6 condition of approximately 200 milliseconds.

### 3 NUMERICAL METHODOLOGY

The transient aerothermoelastic response of the panel is solved by numerically integrating a coupled, nonlinear system of Ordinary Differential Equations (ODEs) based on a Galerkin modal discretisation of the structure and its thermal field.

#### 3.1 Governing Equations and Spatial Discretisation

The structural dynamics of the panel are modelled using nonlinear von Kármán plate theory with for membrane stretching. The panel's transverse deflection,  $w(x, y, t)$ , is approximated as a finite series of  $N_s$  assumed *in-vacuo* eigenmodes based on the specified boundary conditions (i.e., clamped-free-clamped-free). A similar expansion is used to discretise the 2D transient heat conduction equation for the panel's physical temperature field,  $T(x, y, t)$ . Fully-free eigenmodes are used as the basis functions which approximates conductively insulated conditions.

Applying the Galerkin method reduces the governing PDEs to a coupled set of first- and second-order ODEs. These are formulated in state-space form  $\dot{\mathbf{y}} = \mathbf{f}(t, \mathbf{y})$ , where the state vector  $\mathbf{y}$  is defined as:

$$\mathbf{y} = \begin{Bmatrix} \mathbf{q}_s \\ \mathbf{q}_T \\ \dot{\mathbf{q}}_s \end{Bmatrix} \quad (1)$$

##### 3.1.1 Structural Sub-system

The structural equations of motion are solved for the modal accelerations,  $\ddot{\mathbf{q}}_s$ :

$$\mathbf{M}_s \ddot{\mathbf{q}}_s = \mathbf{F}_{\text{gen}}(t, \mathbf{y}) \quad (2)$$

where  $\mathbf{M}_s$  is the structural generalised mass matrix (identity matrix) and  $\mathbf{F}_{\text{gen}}$  is the total generalised force vector.

##### 3.1.2 Thermal Sub-system

The thermal equations are solved for the rate of change of the thermal coordinates,  $\dot{\mathbf{q}}_T$ :

$$\mathbf{C}_T \dot{\mathbf{q}}_T + \mathbf{K}_T \mathbf{q}_T = \mathbf{Q}_{\text{gen}}(t, \mathbf{y}) \quad (3)$$

where  $\mathbf{C}_T$  and  $\mathbf{K}_T$  are the generalised thermal capacitance and conductance matrices, respectively. The generalised thermal capacitance matrix,  $\mathbf{C}_T$ , is derived from the panel's heat capacity. The generalised thermal conductance matrix,  $\mathbf{K}_T$ , is derived from Fourier's law of heat conduction, assuming uniform conductivity  $k_c$ .

### 3.2 System Forcing and Coupling

The system is one-way coupled from the thermal domain to the structural domain. The thermal state critically influences the structural stiffness, but the structural deflection is assumed not to influence the aerodynamic heating.

#### 3.2.1 Inviscid Shock Impingement Model

The discontinuous flow field on the top surface is modelled as a planar, two-dimensional shock-reflection problem by applying the ideal, inviscid oblique shock relations twice. This approach captures the sharp, discontinuous jump in static pressure and temperature. It deliberately neglects the complex and computationally expensive viscous-inviscid phenomena.

### 3.2.2 Asymmetric Flow Environment

The flow fields on the top and bottom surfaces are dissimilar. The top flow is spatially non-uniform, as defined by the shock impingement. The bottom flow is treated as spatially uniform.

### 3.2.3 Aerodynamic Forcing

The aerodynamic loads are modelled using a combination of first-order piston theory and second-order Van Dyke theory. The total aerodynamic pressure is split into linear and nonlinear components. The first-order piston theory pressure provides the linear stiffness and damping terms. This is supplemented by a viscous damping matrix,  $\mathbf{C}_{\text{visc}}$ , which accounts for damping effects from the viscous boundary layer. The nonlinear aerodynamic stiffness is derived from the second-order term of Van Dyke's theory.

### 3.2.4 Total Generalised Structural Force

The total generalised force vector in (2) is a summation of all external and internal forces:

$$\mathbf{F}_{\text{gen}} = \mathbf{F}_{\text{static}} - \mathbf{C}_{\text{lin}}\dot{\mathbf{q}}_s - \mathbf{K}_{\text{lin}}\mathbf{q}_s - \mathbf{F}_{\text{nl,struct}} - \mathbf{F}_{\text{nl,aero}} \quad (4)$$

where  $\mathbf{F}_{\text{static}}$  is the generalised static pressure differential,  $\mathbf{C}_{\text{lin}} = \mathbf{C}_{\text{struct}} + \mathbf{C}_{\text{visc}} + \mathbf{C}_{\text{aero,PT}}$ ,  $\mathbf{K}_{\text{lin}}$  is the total time-varying linear stiffness,  $\mathbf{F}_{\text{nl,struct}}$  is the nonlinear von Kármán force, and  $\mathbf{F}_{\text{nl,aero}}$  is the nonlinear aerodynamic force.

### 3.2.5 Aerothermal Heating

The generalised heat flux is calculated by projecting the net physical heat flux onto each thermal mode. The net heat flux is modelled as the linear summation of the convective heat flux from the top surface and the bottom surface. Each convective flux component is calculated independently using Newton's law of cooling with Eckert's reference temperature method, driven by the local adiabatic wall temperature,  $T_{aw}$ . This semi-empirical approach allows the use of simple, incompressible heat transfer correlations by evaluating all fluid properties at a special 'reference' temperature.

For the top surface all freestream properties are implemented as pre-calculated 2D fields using spatial masks. The bottom surface properties are treated as spatially uniform.

### 3.2.6 Thermo-Structural Coupling

The one-way coupling is realised through the time-varying stiffness matrices, which are updated at every time step based on the instantaneous physical temperature field,  $T(x, y, t)$ :

1. **Thermal Buckling:** A non-uniform thermal stress field,  $\mathbf{N}_{\text{thermal}}$ , is calculated based on the panel's stress-free reference temperature,  $T_{\text{ref}}$ :

$$\mathbf{N}_{\text{thermal}}(x, y, t) = \frac{E(T)\alpha_{th}(T)}{1 - \nu} [T(x, y, t) - T_{\text{ref}}] \quad (5)$$

This stress field, combined with any mechanical pre-loads, is used to re-integrate and find the instantaneous thermal buckling matrix,  $\mathbf{K}_{\text{buckling}}(t)$ .

2. **Material Softening:** The linear and nonlinear structural stiffness matrices are scaled by the change in the mean elastic modulus:

$$\mathbf{K}_{\text{struct}}(t) = \mathbf{K}_{\text{struct,ref}} \left[ \frac{\bar{E}(t)}{E_{\text{ref}}} \right] \quad \text{and} \quad \mathbf{K}_{\text{NL}}(t) = \mathbf{K}_{\text{NL,ref}} \left[ \frac{\bar{E}(t)}{E_{\text{ref}}} \right] \quad (6)$$

where  $\bar{E}(t)$  is the mean modulus of the panel at time  $t$ .

The total linear stiffness is thus  $\mathbf{K}_{\text{lin}}(t) = \mathbf{K}_{\text{struct}}(t) + \mathbf{K}_{\text{aero}} + \mathbf{K}_{\text{buckling}}(t)$ .

### 3.3 Numerical Integration

The resulting system of first-order, nonlinear, stiff ODEs,  $\dot{\mathbf{Y}} = f(t, \mathbf{Y})$ , is integrated in time using the `ode15s` solver in MATLAB. This is a variable-step, variable-order solver based on numerical differentiation formulas (NDFs), which is well-suited for stiff problems.

## 4 RESULTS

The results are primarily focused on a convergence assessment of the solver (number of structural modes, the number of thermal modes, uniform grid-size), with subsequent experimental comparison. These are all conducted at the Mach 6 run condition of TUSQ with the shock generator at a 10-degree incidence. The specific thermostructural state of the panel for experimental comparison is free-expansion to 175° C, and then a further 15° C restricted expansion to a final 190° C. This is effectively thermal buckling due to a  $\Delta T = 15^\circ \text{ C}$ . This model is in support of an AOARD grant, and has use to the Aeroelastic Prediction Workshop High-Speed Working Group.